Symbiotic nutrient cycling enables the long-term survival of Aiptasia in the absence of heterotrophic food sources

Nils Rädecker[1*], Anders Meibom[1,2]

[1] Laboratory for Biological Geochemistry, School of Architecture, Civil and Environmental Engineering, École Polytechnique Fédérale de Lausanne (EPFL), Lausanne, Switzerland

[2] Center for Advanced Surface Analysis, Institute of Earth Sciences, University of Lausanne, Lausanne, Switzerland

* to whom correspondence should be addressed: nils.radecker@epfl.ch

ORCID iDs

Nils Rädecker: 0000-0002-2387-8567

Anders Meibom: 0000-0002-4542-2819

Keywords

Aiptasia | heterotrophy | NanoSIMS | nitrogen limitation | photosymbiosis | Symbiodiniaceae

Author contributions

N.R conceived and conducted the experiment and performed the sample and data analysis. N.R. and A.M. wrote and revised the manuscript.

Conflict of interest

The authors declare no competing interests.

Funding

N.R. and A.M. are supported by the Swiss National Science Foundation, grants 200021_179092 and 205321_212614

Data availability

All associated data are available at zenodo.org.

Abstract

Phototrophic Cnidaria are mixotrophic organisms that can complement their heterotrophic diet with autotrophic nutrients assimilated by their algal endosymbionts. Metabolic models suggest that the translocation of photosynthates and their derivatives from the algae may be sufficient to cover the metabolic energy demands of the host. However, the importance of heterotrophy to the nutritional budget of these holobionts remains unclear. Here, we report on the long-term survival of the photosymbiotic anemone Aiptasia in the absence of heterotrophic food sources. Following one year of heterotrophic starvation, these anemones remained fully viable but showed an 85 % reduction in biomass compared to their regularly-fed counterparts. This shrinking was accompanied by a reduction in host protein content and algal density, indicative of severe nitrogen limitation. Nonetheless, isotopic labeling experiments combined with NanoSIMS imaging revealed that the contribution of autotrophic nutrients to the host metabolism remained unaffected due to an increase in algal photosynthesis and more efficient carbon translocation. Taken together, our results suggest that heterotrophic feeding is not essential to fulfilling the energy requirements of the holobiont on a one-year timescale. But, while symbiotic nutrient cycling effectively retains carbon in the holobiont over long time scales, our data suggest that heterotrophic feeding is a critical source of nitrogen required for holobiont growth under oligotrophic conditions.

Introduction

Photosymbiotic Cnidaria, such as corals and anemones, dominate shallow hard-bottom substrates in the oligotrophic tropical ocean (Pandolfi 2002). The key to their evolutionary and ecological success under these conditions lies in their association with endosymbiotic algae of the family Symbiodiniaceae (Stanley 2006; Stanley and van de Schootbrugge 2009). Efficient nutrient exchange in these symbioses couples the heterotrophic metabolism of the host with the autotrophic metabolism of their algal symbionts (Yellowlees et al. 2008; Cunning et al. 2017). Consequently, photosymbiotic Cnidaria are considered mixotrophic as they can acquire nutrients via heterotrophy and autotrophy alike (Fox et al. 2018; Radice et al. 2019). Under oligotrophic conditions, this confers an ecological advantage that enables these animals to outcompete other benthic organisms restricted to either heterotrophic or autotrophic nutrient sources (Muscatine and Porter 1977; McCook 2001).

In the stable symbiosis, the algal symbionts translocate a large proportion of their photosynthates in the form of sugars and sterols to their host (Falkowski et al. 1984; Burriesci et al. 2012; Tremblay et al. 2014; Hambleton et al. 2019). This carbon translocation fuels the host metabolism and may be sufficient to cover the host's energy demand under optimal environmental conditions (Davies 1984; Rinkevich 1989; Tremblay et al. 2012). The translocated photosynthates have been referred to as 'junk food' because their low nitrogen content limits their potential for anabolic incorporation (Falkowski et al. 1984; Dubinsky and Jokiel 1994). Hence, the utilization of autotrophic nutrients by both symbiotic partners depends, in part, on their access to inorganic nitrogen sources from the surrounding seawater (Davies 1984; Morris et al. 2019; Rädecker et al. 2021). However, under the oligotrophic conditions that prevail in the tropical ocean inorganic nitrogen availability is limited (O'Neil and Capone 2008).

In contrast, heterotrophic nutrient sources have a proportionally higher nitrogen content allowing efficient anabolic assimilation (Hughes et al. 2010). There is ample evidence demonstrating the nutritional benefits of heterotrophic feeding, e.g., in the form of organic nitrogen or vitamins for both symbiotic partners (Goreau et al. 1971; Porter 1976; Houlbrèque and Ferrier-Pagès 2009). As such, high rates of heterotrophic feeding may enable corals to compensate for reduced autotrophic nutrient availability following bleaching; i.e., the stress-induced breakdown of the cnidarian-algal symbiosis (Grottoli et al. 2006; Anthony et al. 2009). However, as our understanding of potential prey dynamics (e.g., zooplankton abundance) and cnidarian grazing on coral reefs remains limited (Lowe and Falter 2015), the importance of heterotrophic nutrients for sustaining the stable cnidarian-algal symbiosis is less clear.

Here, we performed a starvation experiment using the photosymbiotic sea anemone Aiptasia to study the role of heterotrophic nutrient acquisition in symbiosis. For this, we reared Aiptasia for one year in the absence of any heterotrophic nutrient sources. This permitted us to examine the effects of heterotrophic starvation on the symbiosis in light of the underlying carbon and nitrogen cycling and explore the limits of autotrophic nutrient acquisition in the photosymbiotic Cnidaria.

Material & Methods

Animal husbandry & experimental design

The experiments and measurements were performed on the photosymbiotic cnidarian model organism Aiptasia, i.e., *Exaiptasia diaphana* (Puntin et al. 2022). We used the clonal host line CC7 with its native algal symbiont community dominated by the *Symbiodinium linucheae* strain SSA01 (Sunagawa et al. 2009; Grawunder et al. 2015). Animal cultures were reared in 2 L acrylic food containers filled with artificial seawater (35 PSU, Pro-Reef, Tropic Marin, Switzerland). Artificial seawater was freshly prepared in the dark to minimize any potential microbial contamination. Culture stocks were kept at a constant temperature of 20 ˚C under a 12 h: 12 H light-dark cycle (photosynthetic

active radiation = 50 µE m^{-2} s^{-1}) using an Algaetron 230 incubator (Photo System Instruments, Czech Republic). Animals were fed once a week with freshly hatched *Artemia salina* nauplii (Sanders GSLA, USA) followed by a complete water exchange and removal of biofilms.

For the experiment, all animals were reared under the same conditions as outlined above for one year. However, while half of the animals were fed weekly with *Artemia* nauplii (regularly fed control), the other half was reared in the absence of any food sources (heterotrophically starved). Apart from this, all culturing parameters were kept identical, including the weekly cleaning and water exchange.

Phenotypic characterization

Following the one-year experiment, treatment responses were recorded. First, photos of representative phenotypes for each of the treatments were taken with an OM-1 camera and a 60 mm f2.8 macro objective (OM System, Japan) using identical illumination and exposure settings. Then, three animals were collected from each treatment group, transferred to a pre-weighed 1.5 mL Eppendorf tube, and homogenized in 500 µL Milli-Q water using a PT1200E immersion dispenser (Kinematica, Switzerland).

Host and algal symbiont fractions were immediately separated by centrifugation (3000 g, 3 min) and the host supernatant was transferred into a new pre-weighed 1.5 mL tube, flash-frozen in liquid nitrogen, and stored at -20 °C for later analysis. The algal symbiont pellet was resuspended in 500 µL Milli-Q water and rinsed by one additional centrifugation and resuspension step. Algal symbiont concentrations were quantified in three technical replicates per sample based on cell shape and chlorophyll autofluorescence using a CellDrop cell counter (DeNovix, USA). The protein content in the defrosted host supernatant was quantified in three technical replicates using the Pierce Rapid Gold BCA Protein Assay Kit (Thermo Scientific, USA) according to the manufacturer's instructions. Algal concentrations and host protein content were extrapolated to the initial sample volume and normalized to holobiont biomass. Holobiont biomass was approximated as dry weight. For this, host and symbiont fractions were dried at 45 °C until the weight was stable and the initial weight of empty tubes was subtracted from the final weight. The weight of host and symbiont fractions was corrected for aliquots taken for sample measurements to approximate the dry weight of the holobiont as a whole, i.e., host + symbiont fraction.

Isotope labeling & NanoSIMS imaging

To study treatment effects on symbiotic interactions, we quantified inorganic carbon and nitrogen assimilation and translocation in the symbiosis. For this, three animals from each treatment were transferred to 50 mL glass vials. For isotopic labeling, vials were filled with minimal artificial seawater medium (35 PSU, pH 8.1, 355.6 mM NaCl, 46.2 mM $MgCl_2$, 10.8 mM Na_2SO_4, 9.0 mM $CaCl_2$, 7.9 mM, KCl; (Harrison et al. 1980)) containing 2.5 mM $NaH^{13}CO_3$ and 10 µM $^{15}NH_4Cl$. Animals were incubated for 6 h in the light at their regular culture conditions before being transferred to a fixative solution (2.5 % glutaraldehyde and 1 % paraformaldehyde in 0.1 M Sorensen's phosphate buffer). Samples were fixed for 1 h at room temperature followed by 24 h at 4 °C before being stored in a preservative solution (1 % paraformaldehyde in 0.1 M Sorensen's phosphate buffer) at 4 °C until further processing. Within four days of fixation, samples were dissected and individual tentacles were processed for resin embedding. As such, samples were dehydrated in a series of increasing ethanol concentrations (30 % for 10 min, 50 % for 10 min, 2 x 70 % for 10 min, 3 x 90 % for 10 min, and 3 x 100 % for 10 min) and transferred to acetone (100 % for 10 min). Dehydrated samples were gradually infiltrated with SPURR resin (Electron Microscopy Sciences, USA) at increasing concentrations (25 % for 30 min, 50 % for 30 min, 75 % for 1 h, and 100 % overnight) and the resin was polymerized at 65 °C for 48 h. Embedded samples were cut into semi-thin sections (200 nm) using an Ultracut E ultramicrotome (Leica Microsystems, Germany), transferred onto glow-discharged silicon wafers, and sputter-coated with a 12 nm gold layer using an EM SCD050 (Leica Microsystems).

These samples were analyzed with a NanoSIMS 50L instrument (Hoppe et al. 2013). To remove the metal coating, target sample areas were pre-sputtered for 5 minutes with a primary beam of ca. 6 pA. Data were collected by rastering a 16 keV primary ion beam of ca. 2 pA Cs^+ focused to a spot size of about 150 nm across the sample surface of 40 x 40 µm with a resolution of 256 x 256 pixels and a pixel dwell time of 5 ms. The secondary ions $^{12}C_2^-$, $^{12}C^{13}C^-$, $^{12}C^{14}N^-$, and $^{12}C^{15}N^-$ were simultaneously collected in electron multipliers at a mass resolution of about 9000 (Cameca definition), sufficient to resolve potentially problematic mass interferences. For each sample, seven to eight areas were analyzed in five consecutive image layers. The resulting isotope maps were processed using the ImageJ plug-in OpenMIMS (https://github.com/BWHCNI/OpenMIMS/wiki). Mass images were drift- and dead-time corrected, the individual planes were added and $^{15}N/^{14}N$ maps were expressed as hue-saturation-intensity images, where the color scale represents the isotope ratio. ^{15}N assimilation was recorded as atom % excess (in comparison to unlabeled controls) by drawing regions of interest (ROIs) based on $^{12}C^{14}N^-$ maps around individual symbiont cells as well as gastrodermal tissue (excluding symbiont cells) in each of the images (see data file (Rädecker and Meibom 2022)). Due to the clonal nature of Aiptasia and the identical environmental conditions of animals within the same treatment, individual ROIs were considered independent measurements across animal replicates for the purpose of this study.

Statistical analyses

Treatment effects on phenotypic responses, i.e., biomass, host protein content, and symbiont density, were analyzed using two-sided unpaired Student's *t*-tests. Isotope ratios from NanoSIMS analysis were square root transformed to meet model assumptions and analyzed with linear models (LM) using the respective symbiotic partner (host/symbiont) and treatment (fed/starved) as explanatory variables. To test individual differences between groups LMs were followed up with a Tukey HSD post hoc comparison.

Results

Holobiont biomass loss in the absence of heterotrophic nutrients

After one year of husbandry in the absence of heterotrophic food sources, Aiptasia remained viable but had ceased any detectable asexual propagation via pedal lacerates. Starved animals showed pronounced phenotypic differences compared to their regularly fed counterparts. Specifically, starvation resulted in a reduction in body size, a paler appearance, and a loss of 85 % of their dry weight (Fig. 1A,B; Student's *t*-test, $t = 4.71$, $p = 0.042$). This decline in holobiont biomass was, at least in part, driven by a strong decline in host protein content and algal symbiont density, which both decreased by more than 80 % on average when normalized to holobiont biomass (Fig. 1C,D; for host protein: Student's *t*-test, $t = 5.39$, $p = 0.014$; for algal symbiont density: Student's *t*-test, $t = 3.85$ $p = 0.047$ for algal symbiont densities).

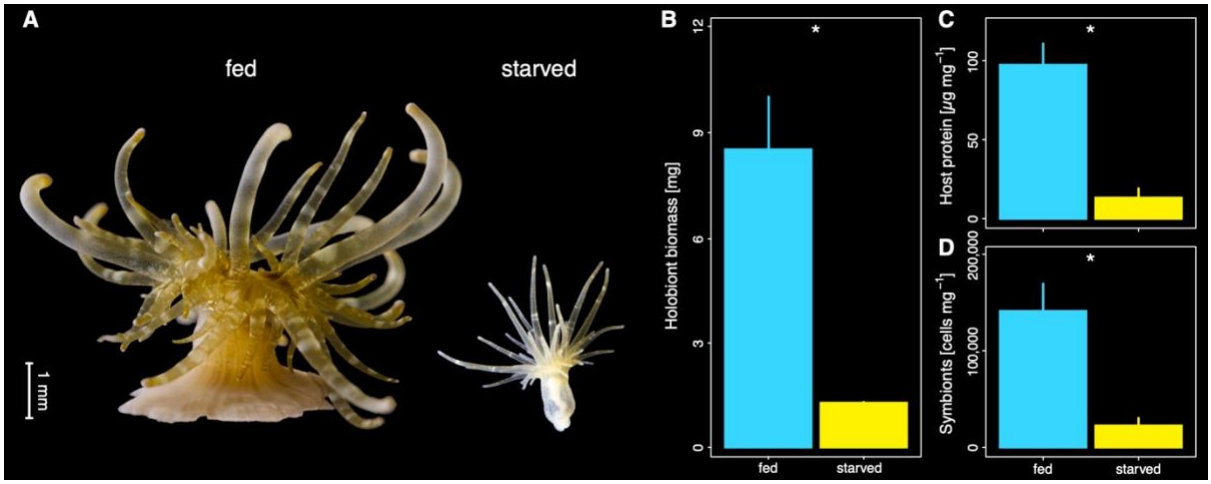

Fig. 1 | Phenotypic response to heterotrophic starvation in Aiptasia. (A) Representative photos illustrating the phenotype of animals that were regularly fed (left) or reared for one year without heterotrophic food sources (right). **(B)** Holobiont biomass expressed as dry weight of fed and starved Aiptasia. **(C)** Protein content of the host tissue per holobiont biomass of fed and starved Aiptasia. **(D)** Algal symbiont density per holobiont biomass of fed and starved Aiptasia. Asterisks indicate significant effects between treatments (*p < 0.05).

Enhanced photosynthetic performance of algal symbionts sustains host metabolism during heterotrophic starvation

NanoSIMS imaging revealed that metabolic interactions in the cnidarian-algal symbiosis remained remarkably stable during heterotrophic starvation despite the pronounced phenotypic response of the Aiptasia holobiont. Consistent with previous reports (Rädecker et al. 2018), ^{13}C enrichment from ^{13}C-bicarbonate assimilation/translocation was highest in the algal symbionts with host ^{13}C enrichment primarily observed in lipid bodies (Fig. 2A,B; host/symbiont differences: LL, F = 666.53, $p < 0.001$). Despite drastic declines in algal symbiont densities during heterotrophic starvation, overall ^{13}C enrichment remained stable in the gastrodermal tissue of the host (Tukey's HSD, $p = 1.000$). This was likely explained by the enhanced photosynthetic performance of algal symbionts reflected in a nearly 50 % increase in their ^{13}C enrichment (Fig. 2C; Tukey's HSD, $p < 0.001$).

The constant availability of photosynthates in the symbiosis during heterotrophic starvation was reflected in the maintained anabolic assimilation of ^{15}N-ammonium by both symbiotic partners. Consistent with previous studies, the algal symbionts acquired the highest ^{15}N enrichments from ammonium assimilation (Pernice et al. 2012; Rädecker et al. 2018), but the host also exhibited clearly measurable ^{15}N enrichments in both epidermal and gastrodermal tissue layers (Fig. 2D,E; host/symbiont differences: LM, F = 660.32, p < 0.001). Thus, heterotrophic starvation did not alter the ability for ammonium assimilation of either symbiotic partner (Fig. 2F; Tukey's HSD, $p = 0.968$ for host gastrodermis, $p = 0.901$ for algal symbionts).

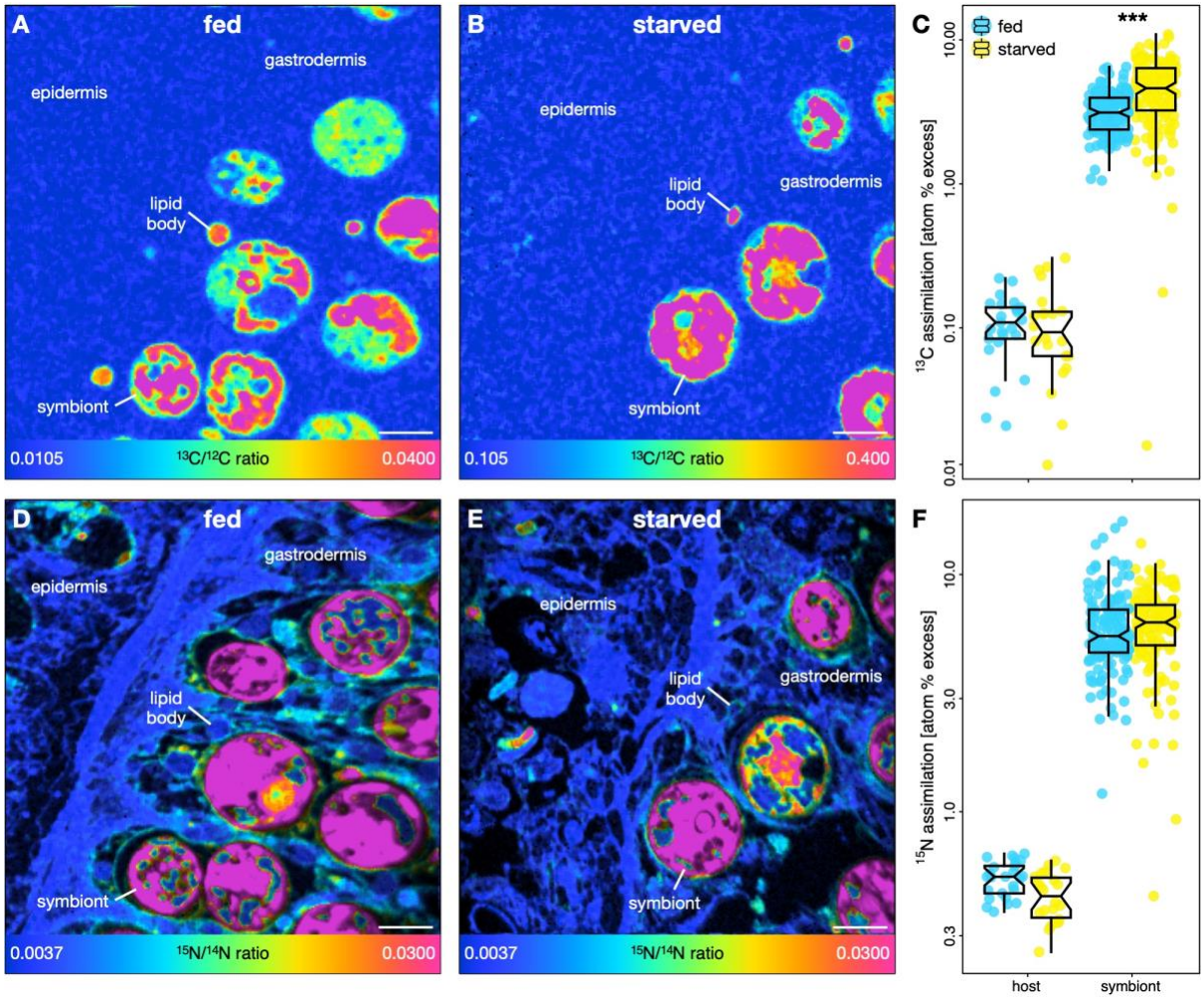

Fig. 2 | NanoSIMS imaging of symbiotic carbon and nitrogen cycling in fed and starved Aiptasia. (A,B) Representative NanoSIMS images illustrating $H^{13}CO_3^-$ assimilation and translocation as $^{13}C/^{12}C$ isotope ratio maps in regularly fed and starved Aiptasia. **(C)** Corresponding boxplots and data points of ^{13}C enrichment for the host gastrodermis and the algal symbiont cells. **(D,E)** Representative NanoSIMS images illustrating $^{15}NH_4^+$ assimilation as $^{15}N/^{14}N$ isotope ratio maps in regularly fed and starved Aiptasia. **(F)** Corresponding boxplots of ^{15}N enrichment for the host gastrodermis and the algal symbiont cells. NanoSIMS ratio maps are shown as hue saturation images with blue representing no/low enrichment and pink representing the highest level of enrichment. Note the logarithmic scale for **C**,**F**. Scale bars are 5 µm. Asterisks indicate significant effects between treatments (***$p < 0.001$).

Discussion

The association with autotrophic endosymbiotic algae has enabled heterotrophic Cnidaria to thrive in the oligotrophic tropical ocean (Muscatine and Porter 1977; Stanley 2006). The long-term starvation experiment presented here emphasizes the remarkable trophic plasticity that this symbiosis confers upon these cnidarian holobionts. Because of the highly efficient symbiotic nutrient exchange and recycling, Aiptasia were able to survive without heterotrophic feeding for at least one year. At the same time, starved animals showed clear signs of nutrient limitation, including reduced biomass, host protein content, and symbiont density, underscoring the long-term importance of heterotrophic feeding for body mass maintenance and growth.

Autotrophic nutrient recycling can sustain the cnidarian-algal symbiosis for extended periods of time

Recent work suggests that the lack of heterotrophic feeding could shift the cnidarian-algal symbiosis towards parasitic interactions that reduce the capacity of the host to survive starvation (Peng et al. 2020). However, here we show that, even after one year of complete heterotrophic starvation, the translocation of photosynthates by algal symbionts remained sufficient to maintain the basal

metabolic requirement of the host. Indeed, patterns of host ^{13}C enrichment (Fig. 2A-C) were not affected by heterotrophic starvation indicating that photosynthate availability for the host was not impaired despite an 85 % reduction in algal symbiont biomass in the holobiont (Fig. 1B). This implies that carbon translocation by individual algal cells must have significantly increased in response to heterotrophic starvation. Indeed, we observed a 50 % increase in ^{13}C enrichment among the algal symbionts in starved animals (Fig. 2C), clearly indicating enhanced photosynthetic performance required for higher relative translocation rates. Similar, albeit less pronounced, trends were previously reported in a three-month starvation experiment using Aiptasia (Davy and Cook 2001). These authors proposed that the increase in algal photosynthetic performance in starved animals was the result of reduced intra-specific competition for CO_2. Indeed, reduced algal symbiont densities likely reduce competition for CO_2 (Rädecker et al. 2017; Krueger et al. 2020). However, in starved animals, this effect could, in part, be masked by the reduced catabolic CO_2 production in the holobiont due to the lack of heterotrophic prey digestion by the host. Our data point to an additional mechanism that could promote enhanced photosynthate release by algal symbionts in the absence of heterotrophy: nitrogen starvation.

Nitrogen limitation shapes the starvation response of Aiptasia

In the stable symbiosis, low nitrogen availability limits the anabolic incorporation of photosynthates in the algal symbiont metabolism (Rädecker et al. 2021; Cui et al. 2022a, 2022b). This nitrogen limitation is thus not only crucial in regulating algal growth but also ensures the translocation of excess photosynthates to the host (Muscatine and Porter 1977; Falkowski et al. 1984). The host passively modulates *in hospite* nitrogen availability for algal symbionts through ammonium assimilation and release in its glutamate metabolism (Rahav et al. 1989; Rädecker et al. 2021; Cui et al. 2022a). Here, we found a proportional decline of algal symbiont density and host protein content in heterotrophically starved Aiptasia. Given that both algal growth and host protein synthesis depend on nitrogen availability, the data suggest that starvation caused severe nitrogen limitation. This is consistent with previous work documenting increases in the carbon-to-nitrogen ratio and lipid content of Symbiodiniaceae in unfed Aiptasia (Cook et al. 1988; Cook and Muller-Parker 1992; Muller-Parker et al. 1996). Strongly reduced nitrogen availability could thus drive the enhanced translocation of photosynthates by the algal symbionts observed here and explain the long-term survival of Aiptasia during heterotrophic starvation.

Interestingly, the reduced nitrogen availability did not cause changes to the ammonium assimilation rates by either symbiotic partner; both continued to efficiently assimilate ammonium from the surrounding seawater in the absence of heterotrophic nutrients. Because ammonium assimilation depends on the availability of carbon backbones from the TCA cycle (Cui et al. 2022b), this observation also suggests that starved holobionts did not experience severe carbon limitation. Yet, the starved holobionts showed severe shrinkage and a significant decline in biomass indicative of malnutrition in the present study. Under the current experimental conditions, environmental ammonium assimilation was thus not sufficient to fulfill the nitrogen requirements of the holobiont. In our experiments, the availability of seawater ammonium was possibly limited by the rate of water exchange (once per week as for the entire animal culture stock). It is thus plausible that higher ammonium concentrations would have allowed the heterotrophically starved Aiptasia to maintain a larger fraction of their original biomass. Yet, in the environmental context of the oligotrophic ocean, photosymbiotic animals are likely similarly limited in their access to environmental ammonium (O'Neil and Capone 2008). In this context, our findings illustrate the importance of heterotrophic feeding by the host for the long-term maintenance of the cnidarian-algal symbiosis biomass. While symbiotic nutrient exchange and recycling may be sufficient to cover the carbon and energy demands of the symbiotic partners on a time scale of at least one year, heterotrophic feeding is not only required for long-term survival but also required for propagation and net growth of the holobiont.

Conclusion

We illustrated the immense trophic plasticity of the cnidarian-algal symbiosis by rearing Aiptasia for an entire year in the complete absence of heterotrophic feeding. Our findings reveal that efficient symbiotic nutrient exchange and recycling are sufficient to sustain the basic metabolic requirements of both symbiotic partners over extended periods of time. Yet, under long-term exposure to highly oligotrophic conditions, the assimilation of environmental inorganic nitrogen will be insufficient to support the nutritional requirements of the holobiont. Heterotrophic feeding thus represents an essential source of nitrogen for holobiont growth. Under oligotrophic conditions, mixotrophy thereby provides a nutritional advantage to photosymbiotic cnidarians that in part explains their ability to outcompete other organisms restricted to either autotrophic or heterotrophic nutrient acquisition.

Acknowledgments

We are grateful to Dr. Claudia Pogoreutz and Gaëlle Toullec for their help with animal culture maintenance. We thank Jean Daraspe for his help with sample processing and Dr. Stéphane Escrig and Florent Plane for their assistance and support with NanoSIMS measurements.

References

Anthony KRN, Hoogenboom MO, Maynard JA, Grottoli AG, Middlebrook R (2009) Energetics approach to predicting mortality risk from environmental stress: a case study of coral bleaching. Funct Ecol 23:539–550

Burriesci MS, Raab TK, Pringle JR (2012) Evidence that glucose is the major transferred metabolite in dinoflagellate--cnidarian symbiosis. J Exp Biol 215:3467–3477

Cook CB, D'Elia CF, Muller-Parker G (1988) Host feeding and nutrient sufficiency for zooxanthellae in the sea anemone *Aiptasia pallida*. Mar Biol 98:253–262

Cook CB, Muller-Parker G (1992) Ammonium enhancement of dark carbon fixation and nitrogen limitation in symbiotic zooxanthellae: effects of feeding and starvation of the sea anemone *Aiptasia pallida* . Limnology and 37:131–139

Cui G, Liew YJ, Konciute MK, Zhan Y, Hung S-H, Thistle J, Gastoldi L, Schmidt-Roach S, Dekker J, Aranda M (2022a) Nutritional control regulates symbiont proliferation and life history in coral-dinoflagellate symbiosis. BMC Biol 20:103

Cui G, Mi J, Moret A, Zhong H, Hung S-H, Al-Babili S, Aranda M (2022b) Nitrogen competition is the general mechanism underlying cnidarian-Symbiodiniaceae symbioses. bioRxiv 2022.06.30.498212

Cunning R, Muller EB, Gates RD, Nisbet RM (2017) A dynamic bioenergetic model for coral-*Symbiodinium* symbioses and coral bleaching as an alternate stable state. J Theor Biol 431:49–62

Davies PS (1984) The role of zooxanthellae in the nutritional energy requirements of*Pocillopora eydouxi*. Coral Reefs 2:181–186

Davy S, Cook C (2001) The relationship between nutritional status and carbon flux in the zooxanthellate sea anemone *Aiptasia pallida*. Mar Biol 139:999–1005

Dubinsky Z, Jokiel PL (1994) Ratio of energy and nutrient fluxes regulates symbiosis between zooxanthellae and corals. Pacific Science 48:313–324

Falkowski PG, Dubinsky Z, Muscatine L, Porter JW (1984) Light and the bioenergetics of a symbiotic coral. Bioscience 34:705–709

Fox MD, Williams GJ, Johnson MD, Radice VZ, Zgliczynski BJ, Kelly ELA, Rohwer FL, Sandin SA, Smith JE (2018) Gradients in primary production predict trophic strategies of mixotrophic corals across spatial scales. Curr Biol 28:3355–3363.e4

Goreau TF, Goreau NI, Yonge CM (1971) Reef corals: autotrophs or heterotrophs? Biol Bull 141:247–260

Grawunder D, Hambleton EA, Bucher M, Wolfowicz I, Bechtoldt N, Guse A (2015) Induction of gametogenesis in the cnidarian endosymbiosis model *Aiptasia* sp. Sci Rep 5:15677

Grottoli AG, Rodrigues LJ, Palardy JE (2006) Heterotrophic plasticity and resilience in bleached corals. Nature 440:1186–1189

Hambleton EA, Jones VAS, Maegele I, Kvaskoff D, Sachsenheimer T, Guse A (2019) Sterol transfer by atypical cholesterol-binding NPC2 proteins in coral-algal symbiosis. Elife 8:

Harrison PJ, Waters RE, Taylor FJR (1980) A broad spectrum artificial sea water medium for coastal and open ocean phytoplankton. J Phycol 16:28–35

Hoppe P, Cohen S, Meibom A (2013) NanoSIMS: Technical aspects and applications in cosmochemistry and biological geochemistry.

316 Geostandards and Geoanalytical Research 37:111–154

317 Houlbrèque F, Ferrier-Pagès C (2009) Heterotrophy in tropical scleractinian corals. Biol Rev Camb Philos Soc 84:1–17

318 Hughes AD, Grottoli AG, Pease TK, Matsui Y (2010) Acquisition and assimilation of carbon in non-bleached and bleached corals. Mar Ecol
319 Prog Ser 420:91–101

320 Krueger T, Horwitz N, Bodin J, Giovani M-E, Escrig S, Fine M, Meibom A (2020) Intracellular competition for nitrogen controls dinoflagellate
321 population density in corals. Proc Biol Sci 287:20200049

322 McCook L (2001) Competition between corals and algal turfs along a gradient of terrestrial influence in the nearshore central Great Barrier
323 Reef. Coral Reefs 19:419–425

324 Morris LA, Voolstra CR, Quigley KM, Bourne DG, Bay LK (2019) Nutrient Availability and Metabolism Affect the Stability of Coral–
325 Symbiodiniaceae Symbioses. Trends Microbiol 27:678–689

326 Muller-Parker G, Lee KW, Cook CB (1996) Changes in the ultrastructure of symbiotic zooxanthellae (*Symbiodinium* sp., Dinophyceae) in fed
327 and starved sea anemones maintained under high and low light. Journal of Phycology 32:987–994

328 Muscatine L, Porter JW (1977) Reef corals: mutualistic symbioses adapted to nutrient-poor environments. Bioscience 27:454–460

329 O'Neil JM, Capone DG (2008) Nitrogen cycling in coral reef environments. Nitrogen in the marine environment. Elsevier New York, pp 949–
330 989

331 Pandolfi J (2002) Coral community dynamics at multiple scales. Coral Reefs 21:13–23

332 Peng S-E, Moret A, Chang C, Mayfield AB, Ren Y-T, Chen W-NU, Giordano M, Chen C-S (2020) A shift away from mutualism under food-
333 deprived conditions in an anemone-dinoflagellate association. PeerJ 8:e9745

334 Pernice M, Meibom A, Van Den Heuvel A, Kopp C, Domart-Coulon I, Hoegh-Guldberg O, Dove S (2012) A single-cell view of ammonium
335 assimilation in coral–dinoflagellate symbiosis. ISME J 6:1314–1324

336 Porter JW (1976) Autotrophy, heterotrophy, and resource partitioning in Caribbean reef-building corals. Am Nat 110:731–742

337 Puntin G, Sweet M, Fraune S, Medina M, Sharp K, Weis VM, Ziegler M (2022) Harnessing the power of model organisms to unravel microbial
338 functions in the coral holobiont. Microbiol Mol Biol Rev e0005322

339 Rädecker N, Meibom A (2022) Data for "Symbiotic nutrient cycling enables the long-term survival of Aiptasia in the absence of heterotrophic
340 food sources."

341 Rädecker N, Pogoreutz C, Gegner HM, Cárdenas A, Roth F, Bougoure J, Guagliardo P, Wild C, Pernice M, Raina J-B, Meibom A, Voolstra CR
342 (2021) Heat stress destabilizes symbiotic nutrient cycling in corals. Proc Natl Acad Sci U S A 118:

343 Rädecker N, Pogoreutz C, Wild C, Voolstra CR (2017) Stimulated Respiration and Net Photosynthesis in Cassiopeia sp. during Glucose
344 Enrichment Suggests in hospite CO2 Limitation of Algal Endosymbionts. Front Mar Sci 4:16

345 Rädecker N, Raina J-B, Pernice M, Perna G, Guagliardo P, Kilburn MR, Aranda M, Voolstra CR (2018) Using Aiptasia as a model to study
346 metabolic interactions in cnidarian-*Symbiodinium* symbioses. Front Physiol 9:214

347 Radice VZ, Brett MT, Fry B, Fox MD, Hoegh-Guldberg O, Dove SG (2019) Evaluating coral trophic strategies using fatty acid composition and
348 indices. PLoS One 14:e0222327

349 Rahav O, Dubinsky Z, Achituv Y, Falkowski PG, Smith DC (1989) Ammonium metabolism in the zooxanthellate coral, *Stylophora pistillata*.
350 Proceedings of the Royal Society of London B Biological Sciences 236:325–337

351 Rinkevich B (1989) The contribution of photosynthetic products to coral reproduction. Mar Biol 101:259–263

352 Stanley GD Jr (2006) Photosymbiosis and the evolution of modern coral reefs. Science 312:857–858

353 Stanley GD, van de Schootbrugge B (2009) The evolution of the coral–algal symbiosis. In: van Oppen M.J.H., Lough J.M. (eds) Coral bleaching:
354 patterns, processes, causes and consequences. Springer Berlin Heidelberg, Berlin, Heidelberg, pp 7–19

355 Sunagawa S, Wilson EC, Thaler M, Smith ML, Caruso C, Pringle JR, Weis VM, Medina M, Schwarz JA (2009) Generation and analysis of
356 transcriptomic resources for a model system on the rise: the sea anemone *Aiptasia pallida* and its dinoflagellate endosymbiont. BMC
357 Genomics 10:258

358 Tremblay P, Grover R, Maguer JF, Hoogenboom M, Ferrier-Pagès C (2014) Carbon translocation from symbiont to host depends on irradiance
359 and food availability in the tropical coral Stylophora pistillata. Coral Reefs 33:1–13

360 Tremblay P, Grover R, Maguer JF, Legendre L, Ferrier-Pagès C (2012) Autotrophic carbon budget in coral tissue: a new ^{13}C-based model of
361 photosynthate translocation. J Exp Biol 215:1384–1393

362 Yellowlees D, Rees TAV, Leggat W (2008) Metabolic interactions between algal symbionts and invertebrate hosts. Plant Cell Environ 31:679–
363 694